

Flow Control in Vehicle Platooning

Internship Case Study



UNIVERSITAT POLITÈCNICA
DE CATALUNYA
BARCELONATECH

Student: **Nadim Saridar**

September 2, 2020

Supervisor: **Dr. Matteo Giacomini**

Contents

1	Introduction	2
2	Problem Setup	2
2.1	Modeling Equations	2
2.2	Computational Domain With Boundary and Initial Conditions	3
2.3	Meshing	4
3	Results	5
3.1	One Body	5
3.2	Two Close Bodies	9
3.3	Two Far Bodies	12
4	Conclusion	16
5	References	17

1 Introduction

Vehicle platooning is the idea of two or more vehicles to travel at the same high speed at a safe distance following each other. Other than being a safety measure, it also helps in changing the flow properties for the vehicles behind the first one that can lead to better fuel economy.

In this study, one vehicle will be tested alone using an Ahmed body, and then a small jet will be added after the slant of the body and see its effects. Then an extra body will be placed behind the first one and results will be compared.

2 Problem Setup

Anslys Fluent is used to create the mesh. Then OpenFOAM was used to do the simulation, with the help of text editors to edit the boundary and initial conditions.

2.1 Modeling Equations

The problem under analysis is modelled using the incompressible Reynolds Averaged Navier-Stokes (RANS) equations, that are:

$$\begin{cases} (\mathbf{u} \cdot \nabla) \mathbf{u} - \nabla \cdot ((\nu + \nu_t) \nabla \mathbf{u}) + \nabla p = 0 \\ \nabla \cdot \mathbf{u} = 0 \end{cases} \quad (1)$$

where (\mathbf{u}, p) are the velocity and pressure fields, and ν and $\tilde{\nu}$ are the kinematic and turbulent viscosities respectively. Equation (1) is closed by proper boundary and initial condition.

In order to compute the turbulent viscosity ν_t , the Spalart Allmaras (SA) model is used:

$$\frac{D}{Dt}(\rho \tilde{\nu}) = \nabla \cdot (\rho D_{\tilde{\nu}} \tilde{\nu}) + \frac{C_{b2}}{\sigma_{\nu_t}} \rho |\nabla \tilde{\nu}|^2 + C_{b1} \rho \tilde{S} \tilde{\nu} (1 - f_{t2}) - \left(C_{w1} f_w - \frac{C_{b1}}{\kappa^2} f_{t2} \right) \rho \frac{\tilde{\nu}^2}{d^2} + S_{\tilde{\nu}} \quad (2)$$

where the turbulence viscosity ν_t is calculated through:

$$X = \frac{\tilde{\nu}}{\nu} \quad (3)$$

$$f_{v1} = \frac{\chi^3}{\chi^3 + C_{\nu 1}^3} \quad (4)$$

$$\nu_t = \tilde{\nu} f_{v1} \quad (5)$$

and all the other coefficients have constant values [1].

The RANS equations with the SA model are solved using SimpleFoam solver in OpenFOAM [2].

2.2 Computational Domain With Boundary and Initial Conditions

The initial conditions are taken based on ambient air at 20°C at atmospheric pressure. The Reynolds number of the flow is $Re = 10^6$, therefore the velocity is set to 10m/s to match this Reynolds number.

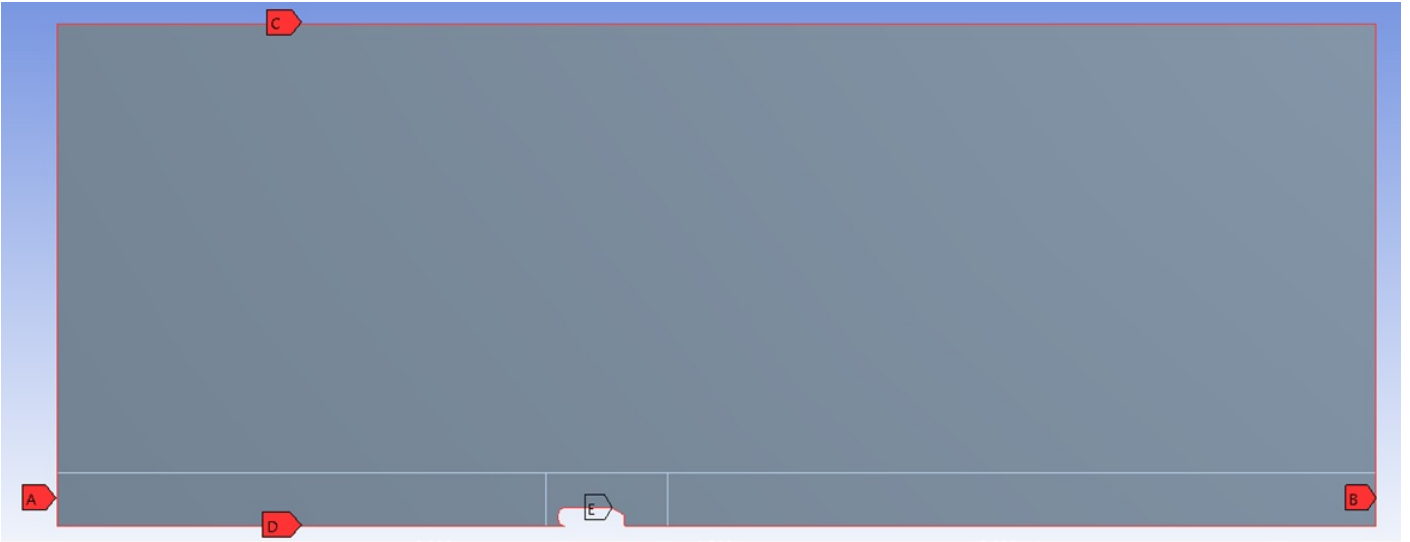


Figure 1: Boundary conditions on one body

As shown in Figure 2, the inlet velocity of the air at (A) is 10m/s . The road and the body are connected and both have the same no slip boundary condition at (D). a zero gradient boundary condition is given to (B). (C) has a symmetry boundary condition.

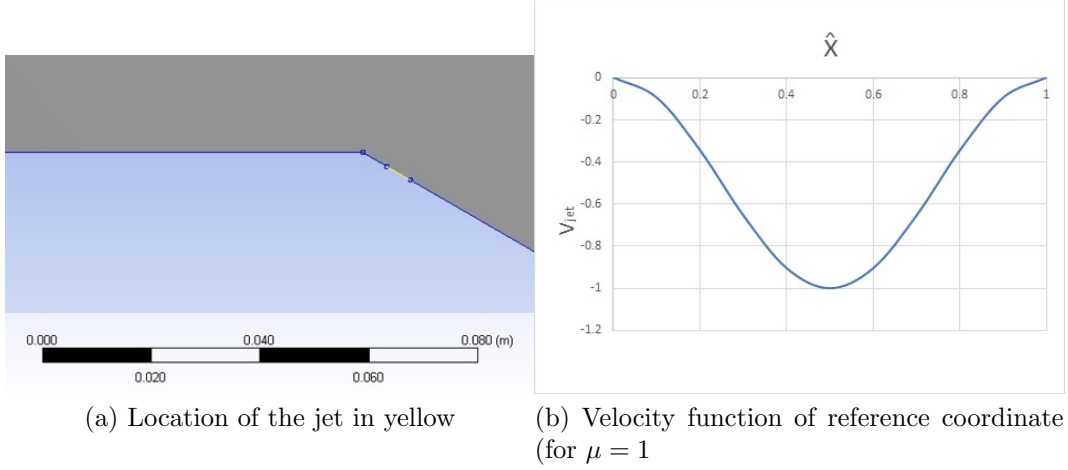


Figure 2: Jet properties

The jet, represented by (E) in the figure, is located 5mm after the slant, and it is 5mm wide. the equation used for the jet is the following:

$$u_{jet}(\hat{x}, \mu) = -\frac{1}{2}\mu(1 - \cos(2\pi\hat{x})) \quad (6)$$

where \hat{x} is the unit width vector following the slant, and μ is the maximum jet velocity. The maximum jet values used are 0, 1, 2.5 and 4m/s .

The same concept was used for two bodies, having the same boundary conditions on the road and both bodies, and both jets having the same equation with the same value of μ .

2.3 Meshing

An assumption was taken before any simulation. This assumption is that the Ahmed body is connected to the road. It was taken to reduce the computations needed to do the simulation because the important results are taken from the upper side of the body where the jet is present. In addition, having the body detached from the road will result with two boundary layers as shown in Figure 1, and a very fine mesh should be used for it to converge, which will result in even more computations.

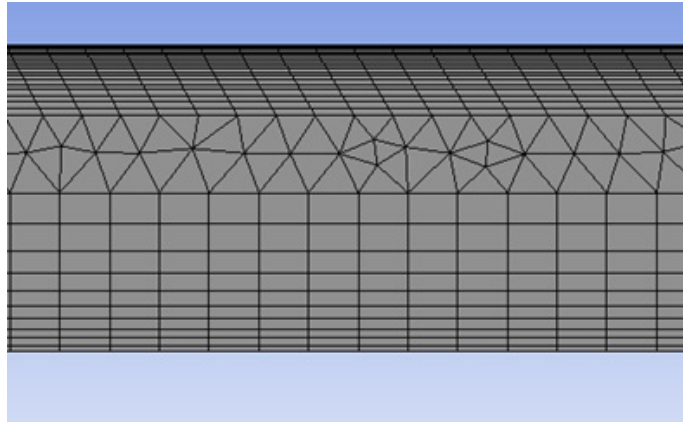


Figure 3: Boundary layers between the road and the body

3 Results

The results are given in the following fashion: first the results with one body are shown to see the effect of the jet, then the results of two close bodies platooning, and lastly two far platooning bodies. The distance between both bodies is given through the following formula: $S = L/x$, where L is the actual distance between the bodies, and x is the length of each body. S has the value of 0.2 for close bodies and 1.6 for far bodies.

All figures shown are postprocessed using Paraview.

3.1 One Body

The drag coefficients in the case of one body have the following values:

Max Jet Value (μ)	Drag Coeff.
0	0.1303
1	0.1282
2.5	0.0923
4	0.0818

Table 1: Drag values for one body

Looking at those results, it is clear that the drag coefficient decreases when the jet velocity increases. However, there is a higher change in values for μ between 1 and 2.5.

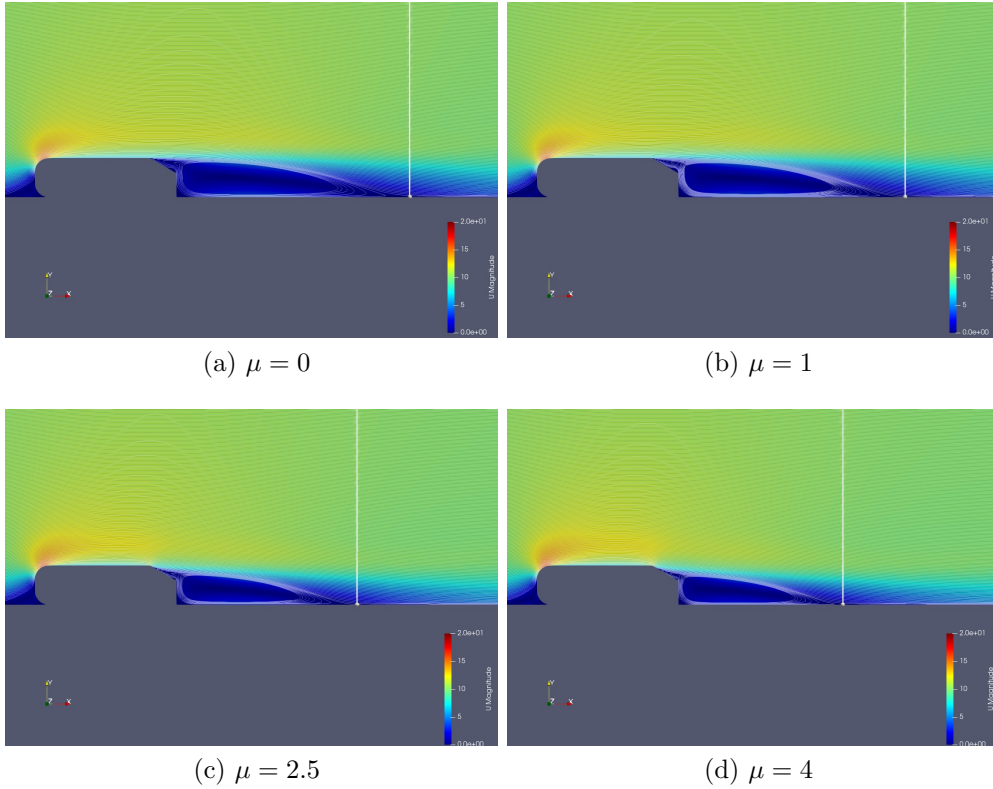


Figure 4: Velocity fields with different values of μ

Max Jet Value (μ)	Reattachment Point
0	1.73
1	1.69
2.5	1.36
4	1.23

Table 2: Reattachement Point for One Body

The vertical lines in figure 4 represent the reattachment point of the flow after the body.

The reattachment point is located where there is a sign change in the wall shear stress after the body. The wall shear stress is computed in OpenFOAM and plotted through a function in Paraview.

Comparing the velocity fields and the reattachment point in figure 4 and table 2, the change is small for values of μ between 0 and 1 in figures 4(a) and 4(b) respectively. However a bigger change is shown in after increasing μ to

2.5. The reattachment point got closer by 20% (table 2) and the recirculation bubble got smaller and shifted a bit downwards as shown in figure 4(c).

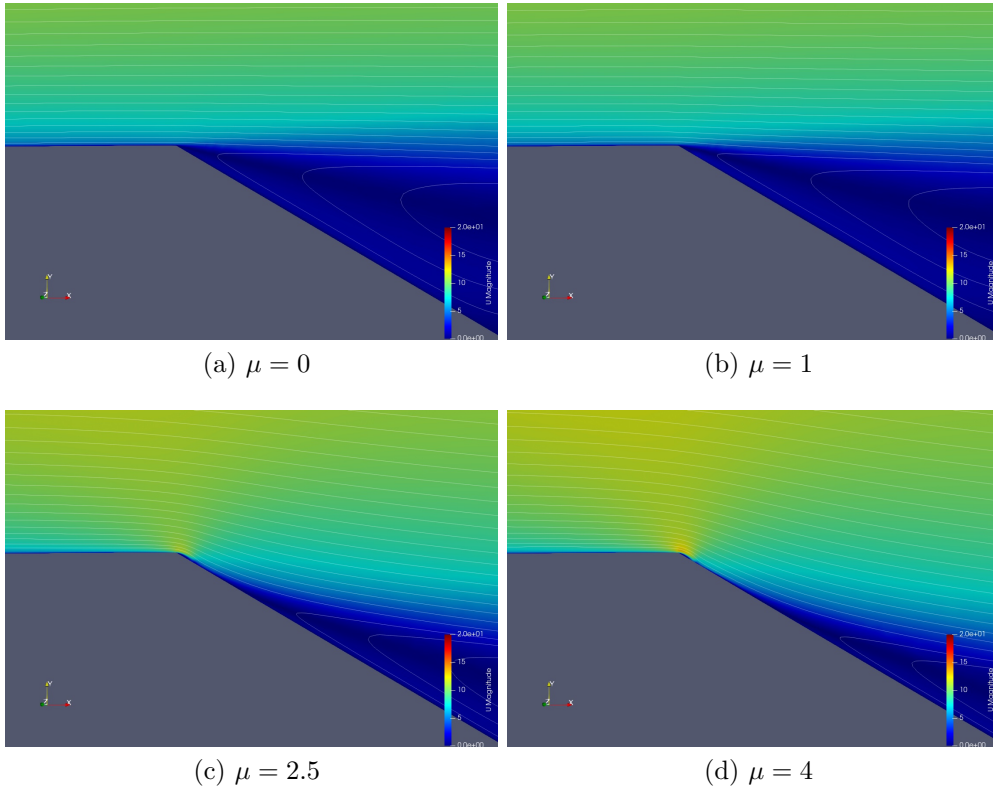


Figure 5: Closer view to velocity fields with different values of μ

Taking a closer look to the velocity fields at the slant, it shows that there is a delay in the detachment of the field at the boundary layer, and it detaches after the slant and after the jet. This explains the change in the recirculation bubble observed above. Therefore a jet with $\mu = 2.5$ is enough to delay the detachment point.

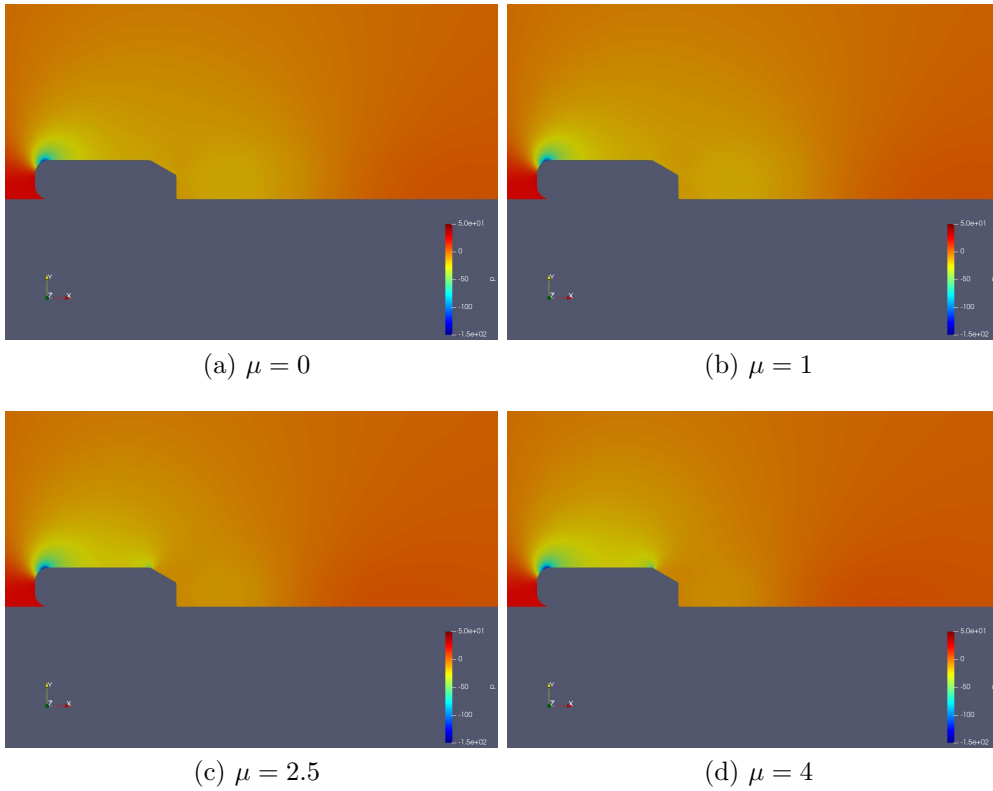


Figure 6: Pressure fields with different values of μ

The results in figure 6 show that the pressure field changes for values of μ between 1 and 2.5. A small low pressure zone appears on the slant for values of μ equal to 2.5 and 4. This low pressure zone appears due to the delay of the detachment of the boundary layer which occurs after the slant, while for values of μ equal to 0 and 1 the detachment of the boundary layer occurs at the slant, as shown in figure 5

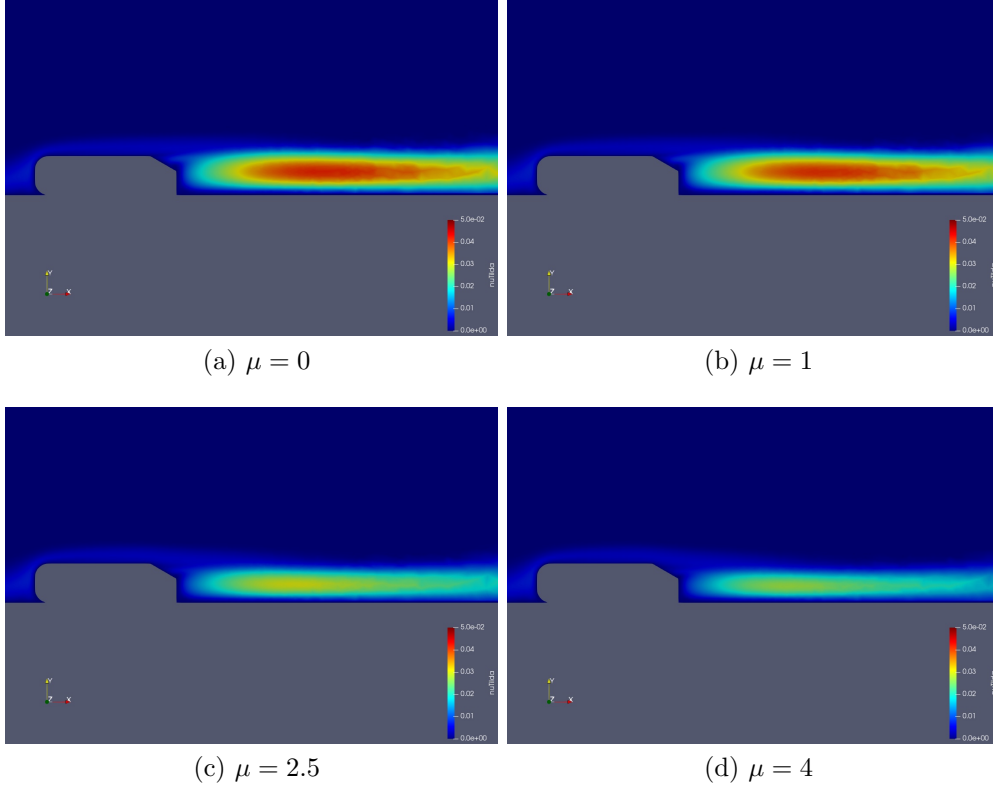


Figure 7: Viscosity fields with different values of μ

Similar to other results, a change is observed for values of μ between 1 and 2.5. for values of μ , the flow after the body becomes less turbulent with lower values of the viscosity.

3.2 Two Close Bodies

In this section, a distance for $S = 0.2$ is taken between the two bodies. Simulations for μ equal to 0 and 1 did not converge. The reason behind it might be because of the assumption taken for the geometry. Therefore the results shown below are for μ equal to 2.5 and 4 for the second body behind the first one.

The drag coefficients are periodic around a mean value for each value of μ .

Max Jet Value (μ)	Minimum	Maximum	Mean
2.5	0.0357	0.0537	0.0447
4	0.0373	0.0528	0.04505

Table 3: Drag values for the second body at a distance $S=0.2$

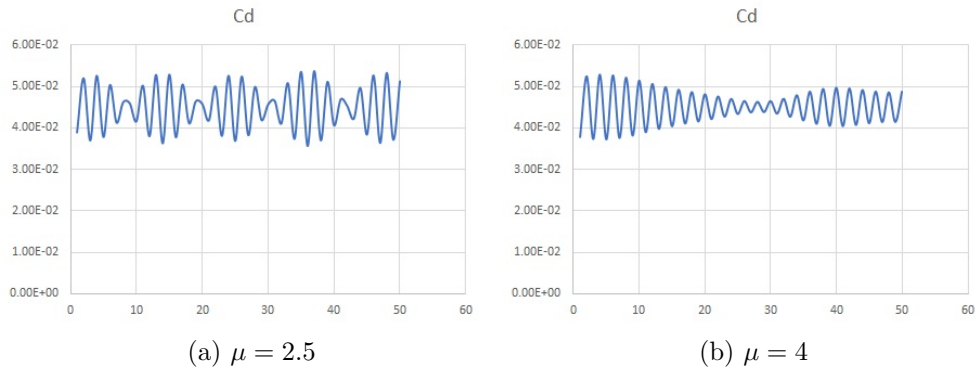


Figure 8: Drag plots with different values of μ for the last 50 iterations

Comparing these results to the ones in table 1, for $\mu = 2.5$ the drag coefficient decreased by around 52%, but for $\mu = 4$ it only decreased by 45%. In addition, the drag coefficient increase for values of μ between 2.5 and 4.

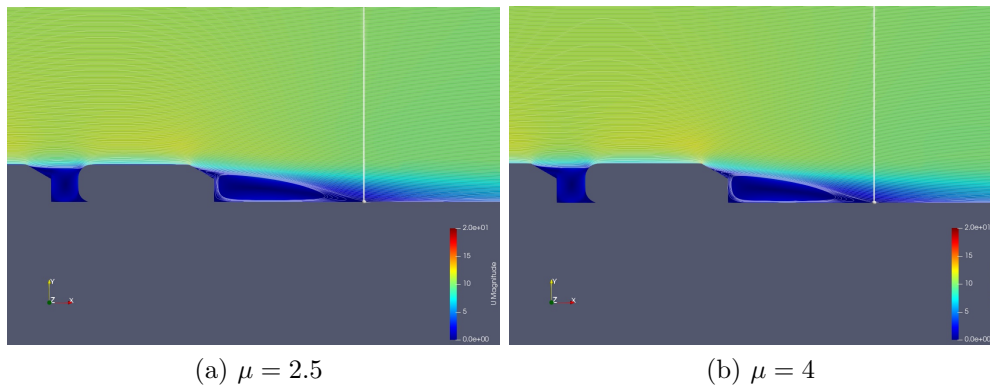


Figure 9: Velocity fields with different values of μ

Max Jet Value (μ)	Reattachment Point
2.5	1.218
4	1.097

Table 4: Reattachment points for two bodies at a distance $S=0.2$

Comparing results of figure 9 and table 4 to the ones in figure 4 and table 2, the reattachment point got closer by around 10.5% for both values of μ , and the recirculation bubbles are smaller. One can notice that for $\mu = 4$ the detachment of the boundary layer is delayed more than the one for $\mu = 2.5$. Therefore the flow from the first body detaches at a lower distance to the ground for higher values of μ .

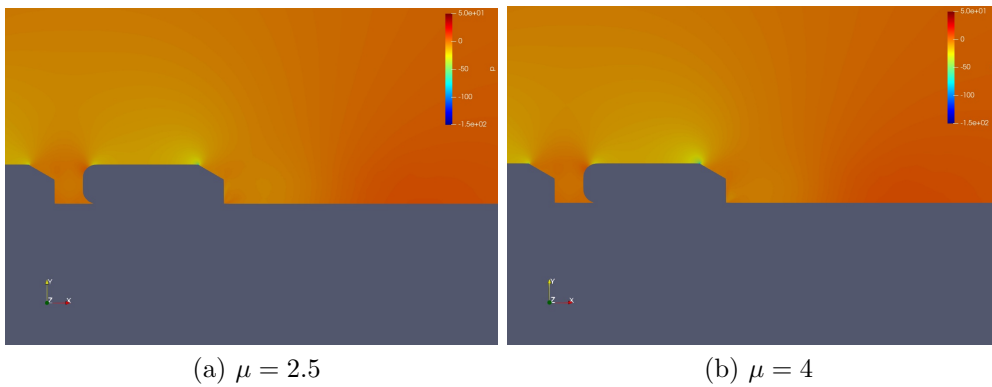


Figure 10: Pressure fields with different values of μ

Due to the delay of the boundary layer from the first body, there is a high pressure zone on the upper front of the second body, therefore the drag will increase, as seen in table 4.

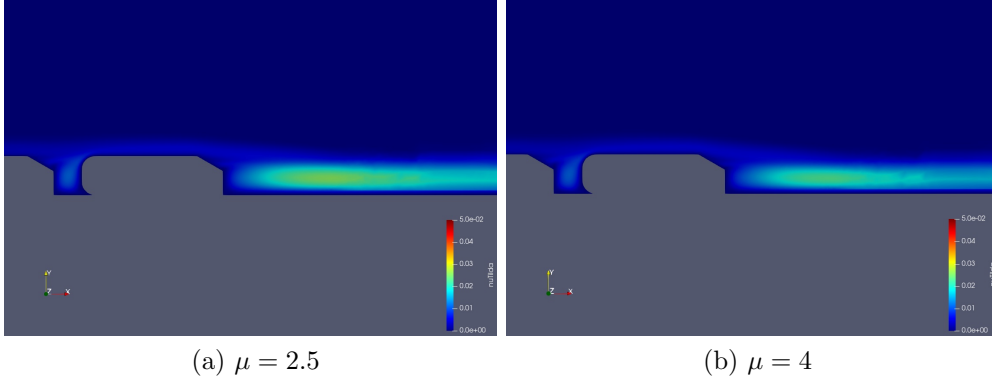


Figure 11: Viscosity fields with different values of μ

Comparing the results to figure 7, the flow is even less viscous than the flow with only one body. In addition, a small viscous zone is present between the two bodies, therefore there is a turbulent flow between the two bodies.

3.3 Two Far Bodies

In this section, a distance for $S = 1.6$ is taken between the two bodies. Simulations for all values of μ converged, and the results shown below are for the second body behind the first one.

The drag coefficients are periodic around a mean value for each value of μ .

Max Jet Value (μ)	Minimum	Maximum	Mean
0	0.0914	0.136	0.1137
1	0.0943	0.135	0.11465
2.5	0.0908	0.118	0.1044
4	0.0957	0.109	0.10235

Table 5: Drag values on the second body at a distance $S=1.6$

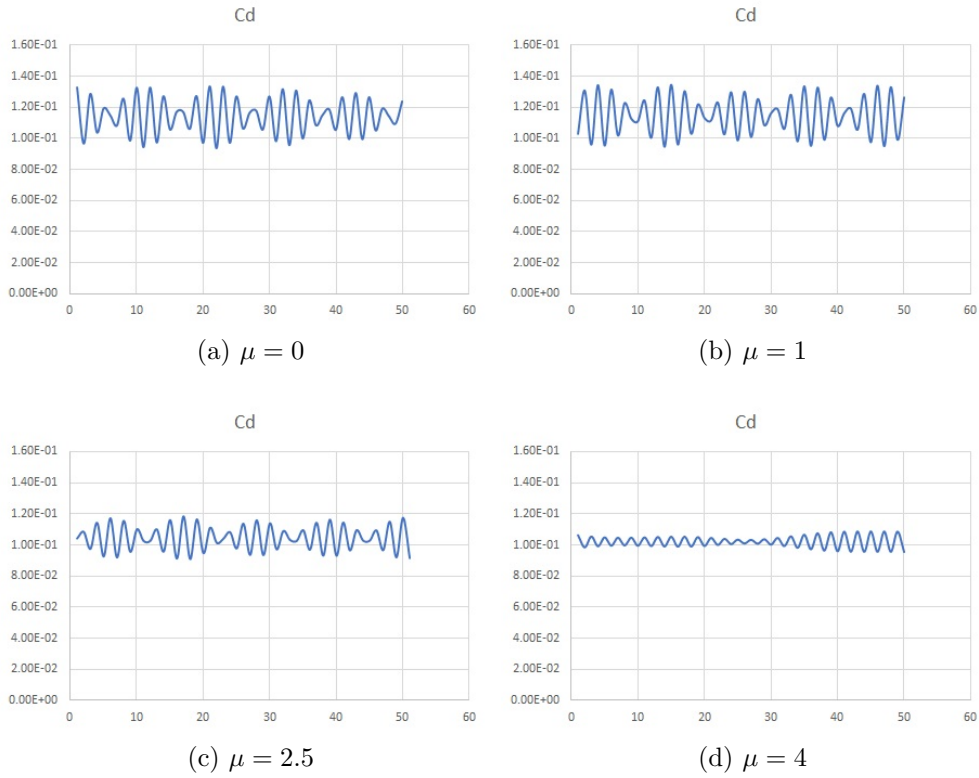


Figure 12: Drag plots with different values of μ for the last 50 iterations

Comparing these results to table 1, there is a reduction in drag of around 12% for μ equal to 0 and 1. However, the drag coefficient increased by 13% and 25% for μ equal to 2.5 and 4 respectively.

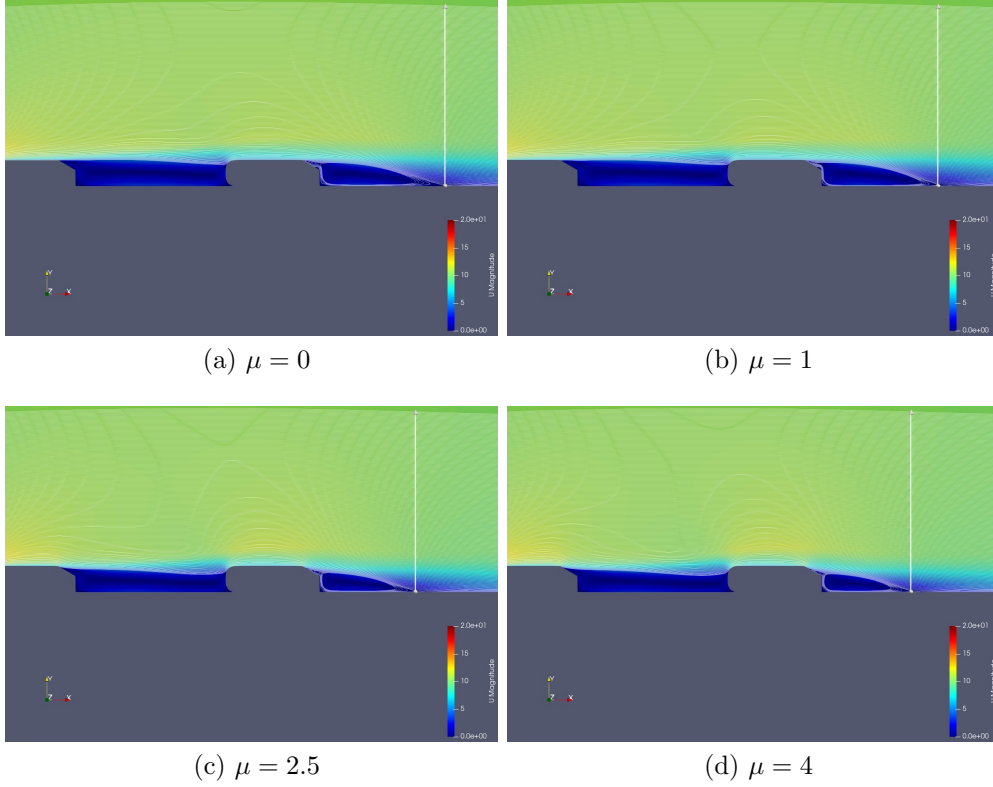


Figure 13: Velocity fields with different values of μ

Max Jet Value (μ)	Reattachment Point
0	1.502
1	1.452
2.5	1.162
4	1.092

Table 6: Reattachment points for two bodies at a distance $S=1.6$

Comparing the results to figure 4 and table 2, the reattachment point got closer and a smaller recirculation bubble is shown for all values of μ . The results are similar to the ones in figure 9 for μ equal to 2.5 and 4. As explained in figure 9, there will be a greater impact from the flow on the second body due to the delay in detachment of the boundary layer from the first body.

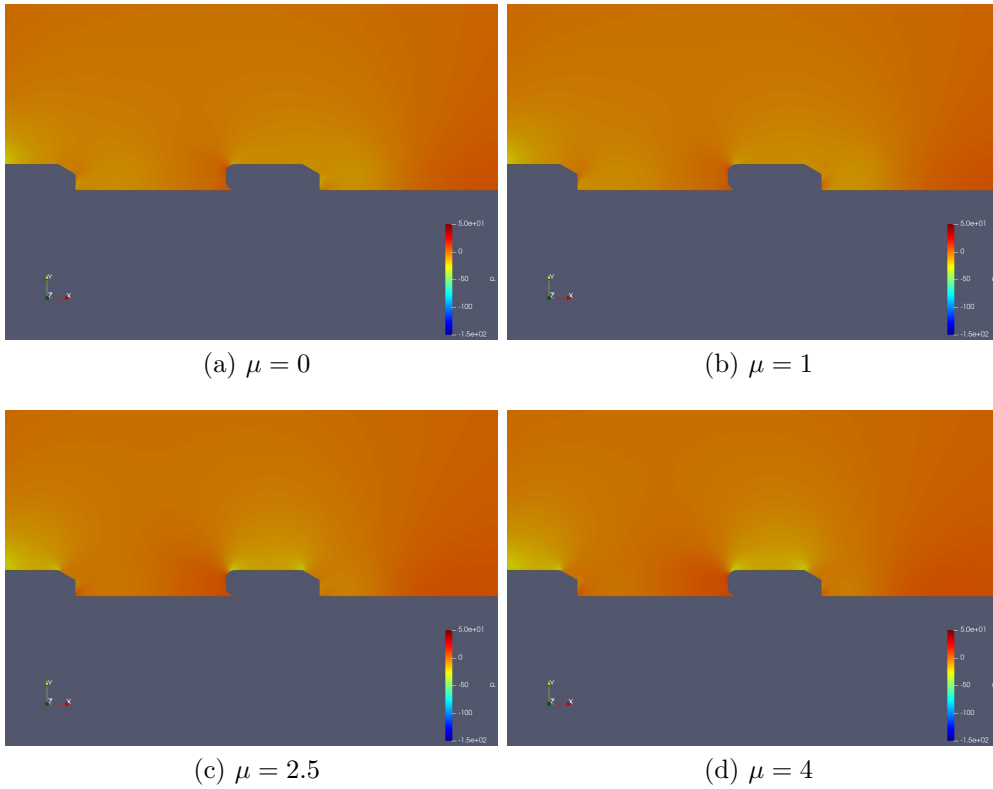


Figure 14: Pressure fields with different values of μ

Due to the delay of the boundary layer from the first body, there is a high pressure zone on the upper front of the second body similar to the one in figure 10, therefore the drag will increase, as seen in table 5 and comparing the values to the ones in table 1.

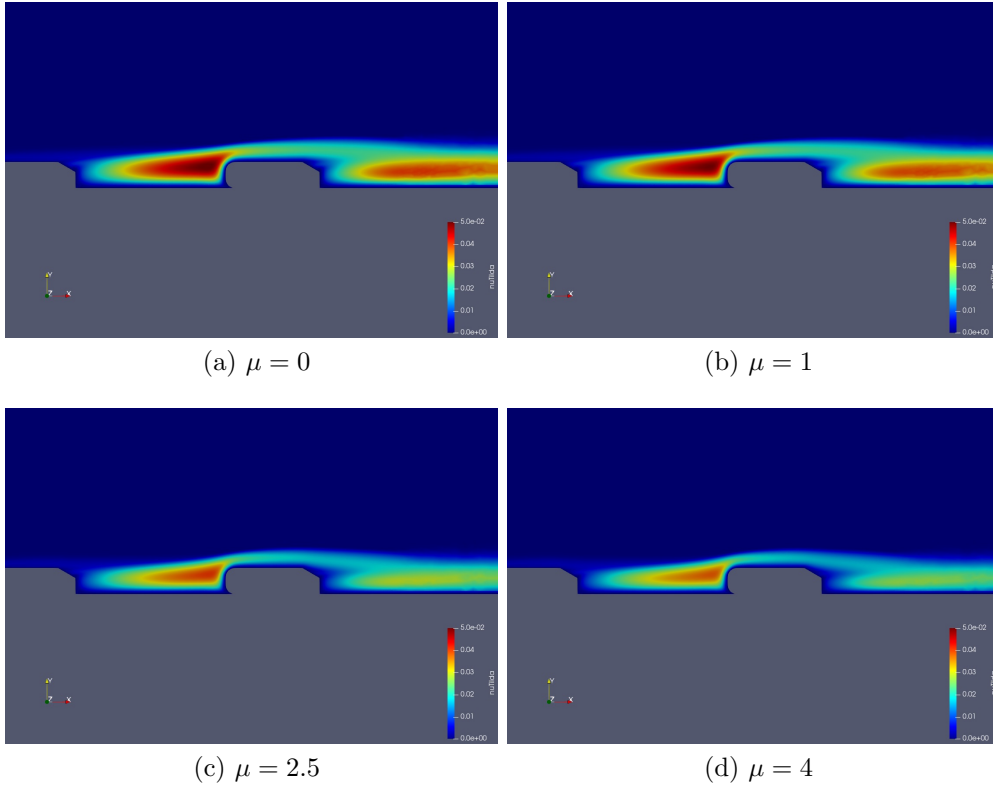


Figure 15: Viscosity fields with different values of μ

Comparing the results to the ones in figure 7, the flow behind the second body is similar to the results of having only one body for all values of μ . However there is a flow with high viscosity between the two bodies for all values of μ . The results for two close bodies in figure 11) are similar, but the two bodies are close enough for that the flow won't be viscous enough.

4 Conclusion

Two parametric studies were performed: one involving the jet and one body, and the other one involving the jet and the distance between two bodies. Interesting results were seen for one body, and varying but improved results were seen for two bodies, after comparing the drag coefficient, the velocity, pressure and viscosity fields.

The platooning did affect the flow on the second body that may improve fuel economy. Further studies could be made on the maximum jet velocity between 1 and 2.5, where a delay in the boundary layer was noticed, and on

the distance between the two bodies where fields could differ.

5 References

[1] Spallart-Allmaras Model: <https://www.openfoam.com/documentation/guides/latest/doc/guide-turbulence-ras-spalart-allmaras.html>

[2] SimpleFoam Solver: <https://www.openfoam.com/documentation/guides/latest/doc/guide-applications-solvers-incompressible-simpleFoam.html>